Electronic structure reconstruction for $\sqrt{3} \times \sqrt{3}$ charge density wave in heavily Cu-intercalated $TiSe_2$ revealed by spatially resolved photoemission spectroscopy

G. Tomassucci,[1] F. Minati,[1] L. Tortora,[1] M. Hattori,[2] A. Barinov,[3] M. Kopciuszynski,[3] S. Kitou,[4] H. Sawa,[5] T. Mizokawa,[2] and N. L. Saini[1]

[1]*Dipartimento di Fisica, Universitá di Roma "La Sapienza" - P. Aldo Moro 2, 00185 Roma, Italia*

[2]*Department of Applied Physics, Waseda University, Shinjuku, Tokyo 169-8555, Japan*

[3]*Sincrotrone Trieste S.C.p.A., Area Science Park, 34012 Basovizza, Trieste, Italy*

[4]*Department of Advanced Materials Science, The University of Tokyo, Kashiwa 277-8561, Japan*

[5]*Department of Applied Physics, Nagoya University, Nagoya 464-8603, Japan*

(Received 20 November 2024; revised 11 November 2025; accepted 2 January 2026; published 23 January 2026)

Scanning photoemission microscopy (SPEM) and angle-resolved photoemission spectroscopy (ARPES) are used to investigate the electronic structure of $Cu_{0.33}TiSe_2$ across the charge density wave (CDW) transition. The electronic structure is found to be largely homogeneous in the normal state above the CDW transition. The ARPES measurements using a submicron beam size reveal a large electronlike pocket due to the Ti *3d* band at the *M* point while the Se 4*p* band at the Γ point is absent due to electron doping by the intercalated Cu. We have observed $\sqrt{3} \times \sqrt{3}$ Fermi surface reconstruction below the CDW transition, in which Ti 3*d* bands are folded into a reconstructed BZ rotated by 30°, making the Γ and *K* points equivalent. The results demonstrate the presence of a $\sqrt{3} \times \sqrt{3}$ CDW phase in the electronic structure of heavily Cu-intercalated $Cu_{0.33}TiSe_2$. The findings reveal a platform for investigating the two-dimensional electronic phase in 1T-$TiSe_2$ chalcogenides, which exhibit a unique interplay between CDW, superconductivity, and excitonic/lattice instabilities.

DOI: 10.1103/dg1f-hm99

I. INTRODUCTION

Highly correlated electron systems are prone to develop different quantum states, such as superconductivity, charge density wave (CDW), or spin density wave (SDW) phases. In particular, a CDW is a spatial modulation of the electron density associated with local lattice distortions, found in many two-dimensional superconductors, including transition metal dichalcogenides (TMDs) [1], intercalated graphite [2], cuprates [3–5], and pnictides [6]. The influence of external parameters such as temperature, pressure, and chemical doping can modulate the underlying interactions, resulting in diverse and complex phase behaviors. It is of particular interest if charge order is competing, cooperating, or simply coexisting with superconductivity [7]. In this context, the question of the origin of the CDW in 1T-$TiSe_2$ provides an interesting case to explore the interplay between these quantum states, thus potentially contributing in resolving similar questions in strongly correlated materials [8–10]. 1T-$TiSe_2$ belongs to the family of TMDs and is often regarded as a unique model system for the study of CDW instability that arises below ∼200 K [11]. The mechanism driving the CDW transition in this system is highly debated, however, the general consensus is that the CDW phase is stabilized by a combination of pseudo-Jahn-Teller effect, supported by the observation of phonon softening [12–14] and excitonic insulator instability manifesting as plasmon softening [15–17].

The recent discovery of superconductivity in Cu_xTiSe_2 [18,19] has further enriched the physics of TMDs. In fact, by applying external pressure, Cu intercalation [20], or substitution of Ti with Ta or Pd [21–23], the CDW transition in 1T-$TiSe_2$ is quickly suppressed and superconducting phase emerges with maximum transition temperature of 4.3 K. The Cu intercalation has large effect on the CDW transition in Cu_xTiSe_2 with the regions of miscibility gaps. In particular, for small Cu intercalation with $x < 0.10$ (so-called β phase), the CDW is characterized by $2 \times 2 \times 2$ ordering. Here, the nesting of the Se 4*p* hole pockets at the Γ (*A*) point and the Ti 3*d* electron pockets at the *M* (*L*) point [24] [see Fig. 1(a)] is suppressed and superconductivity appears. This is followed by a miscibility gap, and a so-called γ_1 phase which appears for $0.18 \leqslant x \leqslant 0.24$ showing an interlayer ordering of Cu with $2 \times 2 \times 2$ reconstruction without any change in the crystal and electronic structure of the $TiSe_2$ layer. With further Cu intercalation, a miscibility gap is followed by a so-called γ_2 phase for $x > 0.30$ showing $\sqrt{3} \times \sqrt{3} \times 2$ CDW, which is different from the original CDW state in nondoped $TiSe_2$ [see Fig. 1(b)] [18,20,25,26]. Superconductivity has not been observed for $x > 0.18$. In contrast to the well-studied Cu_xTiSe_2 for small intercalation, the highly doped regime is not fully explored. In particular, information on the electronic structure of heavily intercalated γ_2 phase of Cu_xTiSe_2 is still missing. Furthermore, one of the open questions to be answered is whether there is a coexistence of CDW and metallic phases

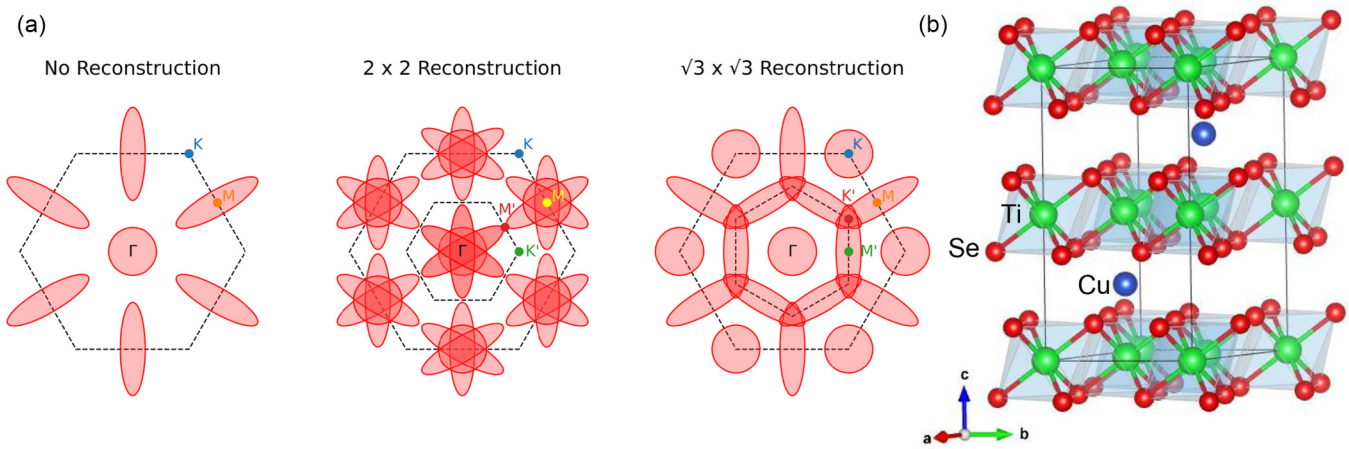

FIG. 1. (a) Schematic pictures of the Fermi surface of 1T-$TiSe_2$ in the normal state (left), 2×2 CDW state (middle), and $\sqrt{3} \times \sqrt{3}$ CDW state (right). In the normal state, the Fermi surface is composed by electronlike pockets at M and holelike pockets at Γ. In the 2×2 CDW state, the bands at M are folded onto Γ and vice versa, giving rise to a flowerlike structure at each M (or equivalently Γ') high-symmetry points. Analogously, in the $\sqrt{3} \times \sqrt{3}$ CDW state, the bands at M are folded into a $\pi/6$-rotated BZ, while Γ and K become equivalent. (b) Crystal structure of $Cu_{0.33}TiSe_2$ illustrated by VESTA [39] for the low temperature γ_2 phase, where interlayer Cu ions are ordered.

due to mobility of intercalated Cu in the same spatial region of the system, or if these phases are distributed in some complex topological order.

Angle resolved photoemission spectroscopy (ARPES) is an ideal tool to study CDW order and many-body interactions, as it provides direct access to the quasiparticle band structure. Earlier ARPES studies on Cu_xTiSe_2 have been focused on small Cu intercalation providing important information on the evolution of electronic structure and CDW across the superconducting dome of this system [27–29]. In conjunction with space resolution ARPES has emerged as a powerful tool in probing the intrinsic electronic structure of quantum materials. Indeed, space-resolved ARPES, combined with scanning photoelectron microscopy (SPEM), has revealed domain-dependent electronic structures of various materials exhibiting coexisting phases at the nanoscale to microscale [30–36]. Here, we have used space-resolved ARPES measurements on $Cu_{0.33}TiSe_2$ across the known CDW transition to address the missing information on the electronic structure at high Cu intercalation in 1T-$TiSe_2$. The ARPES measurements using submicron beam size have permitted us to reveal direct evidence of $\sqrt{3} \times \sqrt{3}$ CDW in the electronic structure of the γ_2 phase of $Cu_{0.33}TiSe_2$. The majority of the system is homogeneous, however, the peculiar Fermi surface reconstruction indicates some electronic inhomogeneity due to mobile Cu atoms. On the other hand, the system exhibits the usual Fermi surface with large electron pockets in the normal phase above the CDW transition temperature. Apart from providing information on the electronic structure of the γ_2 phase, the results show a clear evidence of $\sqrt{3} \times \sqrt{3}$ CDW reconstruction in heavily intercalated 1T-$TiSe_2$ dichalcogenide.

II. EXPERIMENTAL DETAILS

Single crystals of $Cu_{0.33}TiSe_2$ were synthesized following the growth method reported in a previous study [37]. In particular, conventional tube synthesis was employed as the primary technique for preparing polycrystalline samples. These samples were synthesized through the diffusion solid-phase intercalation of metallic copper into the preliminarily synthesized $TiSe_2$. For the intercalation process, a high-purity Cu (99.99%) was utilized. The intercalation reaction was conducted at 950 °C within evacuated (to a residual pressure of 10^{-5} Torr) silica glass tubes. Small copper grains were employed to obtain homogeneous material, and further homogenization was carried out by grinding, mixing, pressing, and subsequent annealing at the same temperature. Single crystals were synthesized using the vapor transport reaction method within evacuated quartz ampoules with the Cu_xTiSe_2 powders served as the initial materials. A flow of substance occurred from the hot (1000 °C) to the cold (600 °C) edge of the ampoule. The resulting single crystals exhibited a platelike morphology with varying size. The amount of Cu in Cu_xTiSe_2 was determined by synchrotron x-ray diffraction (XRD) analysis [38].

The space-resolved ARPES and scanning photoelectron microscopy (SPEM) measurements were carried out at the spectromicroscopy beamline of Elettra synchrotron radiation facility in Trieste, Italy [40]. For the present measurements, linearly polarized light of energy $h\nu = 27$ eV was used, focused using a Schwarzschild optics down to a 500×500 nm^2 beam spot. Fermi surface mapping was carried out by changing the position of electron energy analyzer with the photon beam and the sample position fixed. The sample was cleaved *in situ* at 30 K in ultrahigh vacuum ($<10^{-10}$ mbar) to obtain a clean surface. The total energy resolution was about 50 meV while the angle resolution was 1°. All the measurements were carried out within 12 hours after the sample cleavage.

III. COMPUTATIONAL DETAILS

Density functional theory (DFT) calculations were carried out using the WIEN2k 23.2 code [41] based on the full-potential linearized augmented plane wave plus local orbitals (FP-LAPW + lo) method. The exchange-correlation energy of the electrons was evaluated within the framework of

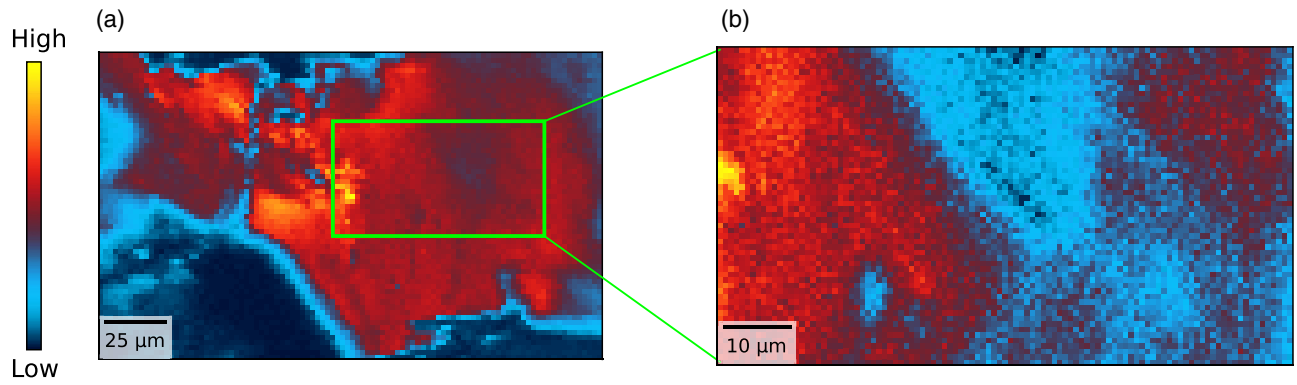

FIG. 2. Scanning photoelectron microscopy (SPEM) maps of $Cu_{0.33}TiSe_2$ measured at 30 K using an incident photon energy of $h\nu = 27$ eV. The maps were acquired with normal emission near the Γ point of the BZ. In particular, (a) represents an overview of the sample with a spatial resolution of $2 \times 2\,\mu m^2$, while (b) is a zoom image on the region bounded by a green rectangle in (a), with the spatial resolution of $1 \times 1\,\mu m^2$. Both images were obtained by integrating photoemission intensities within $-3.0\,\text{eV} \leqslant E - E_F \leqslant 0.2\,\text{eV}$.

the generalized gradient approximation (GGA) as formulated by Perdew, Burke, and Ernzerhof (PBE) [42]. To account for the on-site Coulomb interaction in the Ti $3d$ orbitals, the calculations were performed with an effective Hubbard parameter $U = 3.5$ eV applied to Ti atoms [43,44]. The computations were performed on a supercell of $\sqrt{3} \times \sqrt{3} \times 2$ of $Cu_{0.33}TiSe_2$. The initial crystal structure was taken from diffraction data [38] and subsequently relaxed until all atomic forces were below 0.5 mRy/atom. As such, the valence wave functions within the Muffin-Tin spheres were expanded up to $L\text{max} = 10$ and the charge density was Fourier expanded up to $G\text{max} = 16$. The Brillouin zone for the self-consistent field calculation (scf) was sampled using a $6 \times 6 \times 3k$-point grid, following the Monkhorst-Pack scheme [45]. The energy cut off for the separation of valence and core electrons was set at −6.0 Ry, while the cutoff parameter $R_{\text{MT}}K_{\text{max}}$ was set to 6.5, where R_{MT} is the smallest radius among all atomic spheres, and K_{max} determines the truncation of the reciprocal lattice expansion of the wave functions in the interstitial region. The selected R_{MT} values for Se, Ti, and Cu atoms were 2.35, 2.40, and 2.47 a.u., respectively. The convergence criterion for energy was established at 10^{-4} Ry per unit cell. The unfolded band structure of the supercell was obtained using the fold2Bloch code [46], which allows projection onto the Brillouin zone of the primitive cell. Similar computational details were utilized in a previous study [38].

IV. RESULTS AND DISCUSSIONS

Figure 2 shows SPEM maps measured at 30 K on $Cu_{0.33}TiSe_2$ with normal emission geometry corresponding to the Γ point of the Brillouin zone (BZ). The maps are obtained by integrating photoemission intensities within $-3.0\,\text{eV} \leqslant E - E_F \leqslant 0.2\,\text{eV}$ where $E - E_F$ represents the energy relative to the Fermi level (E_F). The sample has a large flat surface, indicating a very good cleavage. The majority of the sample exhibits a homogeneous electronic structure within the employed space resolution ($2 \times 2\ \mu m^2$). However, some contrast can be seen in the map obtained by doubling the spatial resolution [Fig. 2(b)] indicating electronic inhomogeneity, also evident in Fig. S1 (see the Supplemental Material [47]). This contrast is most likely due to small differences in the spatial distribution of Cu intercalation. Incidentally, electronic inhomogeneities at smaller length scales have been reported by STM experiments on samples with small Cu intercalation, underlining existence of domains that are widespread with increasing Cu [48–50]. Therefore, it may not be surprising to see such electronic domains with small difference in Cu content also in heavily doped system.

In order to investigate the band structure and the Fermiology, we have performed ARPES measurements using submicron beam size (500 nm) on the bright and dark regions of Fig. 2(b). In the parent 1T-$TiSe_2$, one expects to see electronlike bands near the M (or equivalently L) point of the Brillouin zone (BZ) and holelike band near the Γ point [51]. The Fermi surface nesting or excitonic coupling between the electronlike (Ti $3d$) and holelike (Se $4p$) bands drives the system to a $2 \times 2 \times 2$ CDW state with corresponding band folding [see Fig. 1(a)]. The effect of Cu intercalation is to expand the electronlike Ti $3d$ pockets near the M point and to suppress the $2 \times 2 \times 2$ CDW phase.

The segmented ARPES maps at different binding energies are presented in Fig. 3(a). The Fermi surface shape at 30 K, reproduced in Fig. 3(b), is not compatible with a 2×2 CDW phase, nor with the one of the normal phase. Instead, it seems similar to a phase with $\sqrt{3} \times \sqrt{3}$ CDW, where the Ti $3d$ bands are folded onto a reconstructed BZ rotated by 30° with respect to the original, as shown pictorially in Fig. 1(a). Specifically, the original and folded Ti $3d$ bands are supposed to intersect at the K' high-symmetry points of the reconstructed BZ, resulting in missing segments due to suppresion of spectral weight at these points. Apparently, the Fermi surface shape in Fig. 3(b) suggests the system is in $\sqrt{3} \times \sqrt{3}$ CDW phase. Using synchrotron x-ray diffraction, Kitou *et al.* [38] have concluded that the CDW in the γ_2 phase is a cooperative phenomenon with a significant role played by Cu ordering. The findings of this study are consistent with Kitou *et al.* [38]. Indeed, the CDW in the γ_2 phase appears to be multifactorial, with excitonic correlations expected to be diminished due to electron screening. Nevertheless, structural instabilities persist, potentially coupling to the periodic potential introduced by Cu ordering. The ARPES results employing a submicron beam size provide evidence for this scenario: they reveal the coexistence of distinct domains with varying electronic

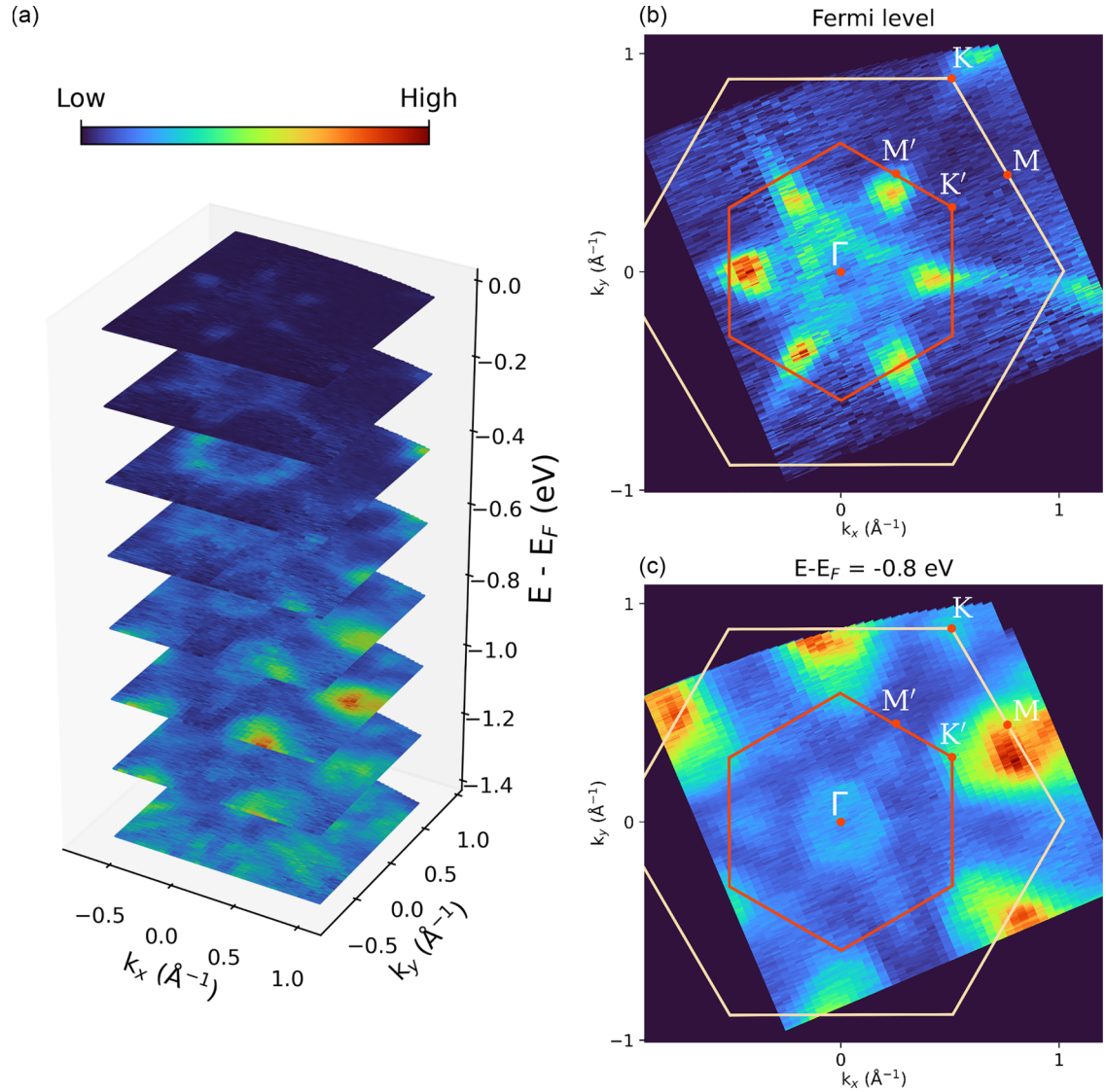

FIG. 3. (a) Series of segmented ARPES intensity maps at different binding energies, obtained using 27 eV photons at 30 K, where the system is in the CDW state. (b) Fermi surface map showcasing a $\sqrt{3} \times \sqrt{3}$ reconstruction of BZ with a peculiar folding of the electronic bands. (c) Intensity at 0.8 eV below the Fermi level. The original BZ is depicted in white, while the reconstructed one is represented in red.

configurations, implying that Cu ordering, lattice fluctuations, and residual correlation effects cooperate to generate a complex, mixed-phase electronic landscape.

The band structure along the $\Gamma - M - K - \Gamma$ cut of the BZ is shown in Fig. 4(a). The measured band structure of $Cu_{0.33}TiSe_2$ seems complex due to large electron doping and $\sqrt{3} \times \sqrt{3}$ CDW reconstruction. Notably, the holelike bands at the Γ points of the BZ are significantly shifted to higher binding energies due to large electron doping from the intercalated Cu. The band structure is largely compatible with a $\sqrt{3} \times \sqrt{3}$ CDW reconstruction, where the holelike bands at Γ are folded onto the K point of the BZ. At E_F, we thus find Se $4p$ bands at Γ and K (which are equivalent due to the reconstruction), while electronlike bands of Ti $3d$ character are found at K'. Below E_F, we can see electronlike bands centered at M, with a minimum located at ~ -1 eV. Additionally, flat bands are noticeable at around -2 eV between the K and M' points.

The measured band structure is largely reproduced by the DFT calculations for $\sqrt{3} \times \sqrt{3}$ CDW reconstruction, depicted in Fig. 4. The majority of the features are well captured, however, there are some bands appearing in the experiment that do not show up in the DFT calculations. The theoretically predicted electron pockets at K' are not observed, suggesting excitonic or lattice fluctuations which are not incorporated in the calculations. In addition, the electronlike band centered at Γ with a minimum around -1.5 eV could not be reproduced in the calculations for a homogeneous phase with x=0.33. Incidentally, DFT calculations for Cu_xTiSe_2 at lower Cu content ($x = 0.11$) shows a clear electronlike band at this energy [52], surviving for x as high as 0.18. Similarly, an electronlike feature along Γ-M', which is absent in the calculation performed for a homogeneous phase, however, is present for heavily intercalated Cu_xTiSe_2 (x=0.5) where local disotortion appear to show an electronlike band [53]. Therefore, it is likely that the bands at Γ with a minimum around -1.5 eV and the

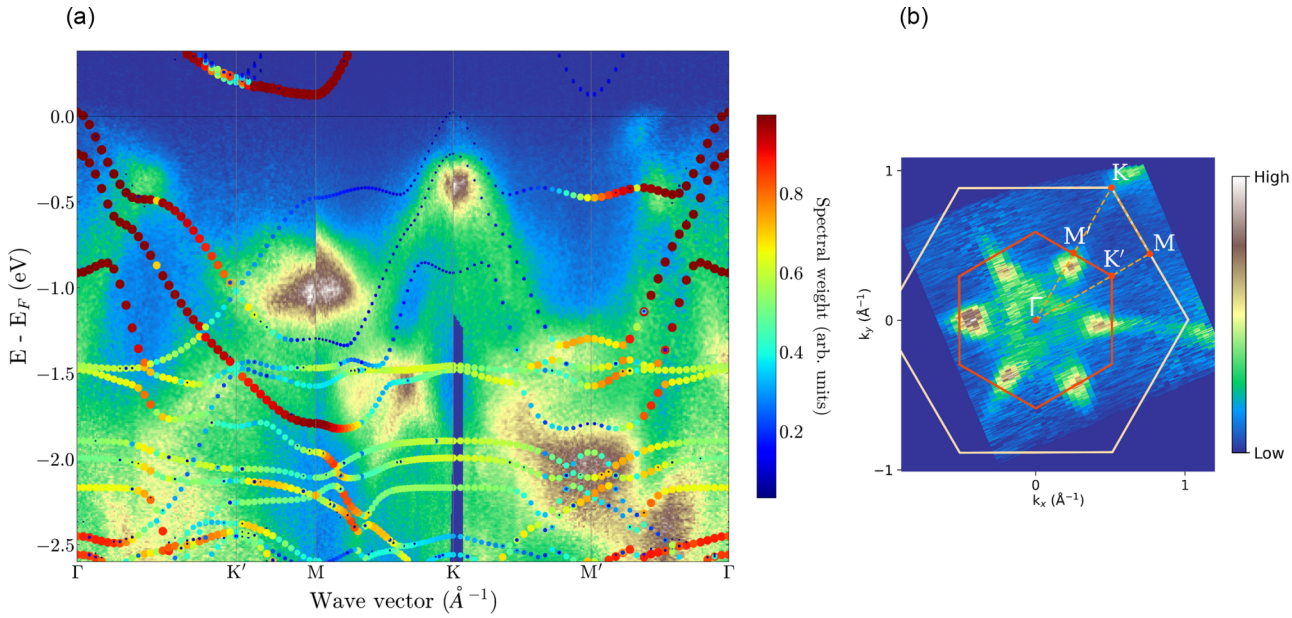

FIG. 4. (a) ARPES spectra of $Cu_{0.33}TiSe_2$ at 30 K along the high-symmetry direction $\Gamma - M - K - \Gamma$ which is shown by an orange dashed curve in (b). The computed band structure is superimposed upon the experimental data. The symbol size is proportional to the spectral weight as shown by the color bar.

spectral weight along Γ-M' near the Fermi level are coming from the coexisting phases at submicron scale with differing Cu content. The inhomogeneity may be justified by the high mobility of the intercalated Cu atoms in the system, leading to various domains within the region illuminated by the beam, each characterized by different Cu concentrations and resulting in different reconstructions. As mentioned earlier, the intrinsic electronic inhomogeneity, has also been seen by a series of STM studies in Cu-intercalated $TiSe_2$ [48–50]. The intrinsic inhomogeneity of Cu distribution was further verified by space resolved micro x-ray absorption spectroscopy (μ-XAS) on the same area of the single crystal measured in this work. Here, we do not rule out a small discrepancy due to surface nature of the observed states as the DFT calculations are performed for a bulk crystal. Nevertheless, it is clear that the majority of the system is in the $\sqrt{3} \times \sqrt{3}$ CDW phase. As such, even though the Fermi surface nesting condition is degraded by the electron doping, the band folding can survive.

In order to explore the electronic structure in the normal state, we have performed the measurements at 250 K. The SPEM images at 250 K (Fig. S2 in the Supplemental Material [47]) appears homogeneous with minimal contributions from bands at the Γ point with majority of the contribution at E_F originating from bands at the M point. The ARPES measurements in the normal state (Fig. S3 in the Supplemental Material [47]) show a Fermi surface dominated by Ti $3d$ bands at the M point, while the Se $4p$ bands at the Γ are absent. The system regains the electronic structure of the pristine $TiSe_2$ [51], however, with the large electron pockets at the M point while the holelike band at Γ are pushed down. We should mention that the same measurements were performed at bright and dark regions, however, within the current energy resolution they led to similar results for the Fermi surface and the band structure (Fig. S3 in the Supplemental Material [47]).

V. CONCLUSIONS

In summary, we have investigated the electronic structure of heavily Cu intercalated Cu_xTiSe_2 by space-resolved photoemission spectroscopy. The ARPES measurements with submicron beam reveals large electron pockets at the M point due to Ti $3d$ orbitals, while the Se $4p$ bands at the Γ point are absent at the Fermi surface consistent with heavy electron doping by the Cu intercalation. In the CDW phase at low temperature we find $\sqrt{3} \times \sqrt{3}$ CDW in $Cu_{0.33}TiSe_2$ with signatures of some electronic inhomogeneity. This suggests a phase where the Ti $3d$ bands are folded into a reconstructed Brillouin zone, rotated by 30 °C, making the Γ and K high symmetry points equivalent. Six Fermi pockets at M' are clearly observed. The comparison with the DFT results suggests possible excitonic or lattice fluctuations. The metallic CDW state identified in the present work is in sharp contrast to the excitonic insulating state in 1T-$TiSe_2$ and provides a playground of two dimensional electronic state with possible excitonic/lattice instabilities.

ACKNOWLEDGMENTS

We thank the E. staff for the assistance during the measurements and for the partial assistance. The work is partially supported by the Sapienza University of Rome and JSPS KAKENHI (No. 19H00659). The work is partially supported by Sapienza University of Rome under the National Recovery and Resilience Plan (NRRP), Mission 4 Component 2 Investment 1 of the Italian Ministry of University and Research (MUR); funded by the European Union - NextGenerationEU - Award No. PE0000021, Concession Decree No. 1561 of 11.10.2022 adopted by the MUR, and CUP B53C22004070006 project title "Network 4 Energy Sustainable Transition - NEST."

DATA AVAILABILITY

The data that support the findings of this article are not publicly available upon publication because it is not technically feasible and/or the cost of preparing, depositing, and hosting the data would be prohibitive within the terms of this research project. The data are available from the authors upon reasonable request.

[1] J. Wilson, F. Di Salvo, and S. Mahajan, Charge-density waves and superlattices in the metallic layered transition metal dichalcogenides, Adv. Phys. **24**, 117 (1975).

[2] K. Rahnejat, C. Howard, N. Shuttleworth, S. Schofield, K. Iwaya, C. Hirjibehedin, C. Renner, G. Aeppli, and M. Ellerby, Charge density waves in the graphene sheets of the superconductor CaC_6, Nat. Commun. **2**, 558 (2011).

[3] C. Howald, H. Eisaki, N. Kaneko, and A. Kapitulnik, Coexistence of periodic modulation of quasiparticle states and superconductivity in $Bi_2Sr_2CaCu_2O_{8+\delta}$, Proc. Natl. Acad. Sci. USA **100**, 9705 (2003).

[4] J. Chang, E. Blackburn, A. Holmes, N. Christensen, J. Larsen, J. Mesot, R. Liang, D. Bonn, W. N. Hardy, A. Watenphul, M. v. Zimmermann, E. M. Forgan, and S. M. Hayden, Direct observation of competition between superconductivity and charge density wave order in $YBa_2Cu_3O_{6.67}$, Nat. Phys. **8**, 871 (2012).

[5] G. Ghiringhelli, M. Le Tacon, M. Minola, S. Blanco-Canosa, C. Mazzoli, N. Brookes, G. De Luca, A. Frano, D. Hawthorn, F. He, T. Loew, M. Moretti Sala, D. C. Peets, M. Saluzzo, E. Schierle, R. Sutarto, G. A. Sawatzky, E. Weschke, B. Keimer, *et al.*, Long-range incommensurate charge fluctuations in (Y, Nd)$Ba_2Cu_3O_{6+x}$, Science **337**, 821 (2012).

[6] E. Rosenthal, E. Andrade, C. Arguello, R. Fernandes, L. Xing, X. Wang, C. Jin, A. Millis, and A. Pasupathy, Visualization of electron nematicity and unidirectional antiferroic fluctuations at high temperatures in NaFeAs, Nat. Phys. **10**, 225 (2014).

[7] B. Keimer, S. Kivelson, M. Norman, S. Uchida, and J. Zaanen, From quantum matter to high-temperature superconductivity in copper oxides, Nature (London) **518**, 179 (2015).

[8] M. Huber, Y. Lin, N. Dale, R. Sailus, S. Tongay, R. Kaindl, and A. Lanzara, Mapping the dispersion of the occupied and unoccupied band structure in photoexcited 1T-$TiSe_2$, J. Phys. Chem. Solids **168**, 110740 (2022).

[9] M. Hattori, G. Tomassucci, G. Hayashi, M. Okawa, M. Kopciuszynski, A. Barinov, Y. Lu, H. Takagi, N. Saini, and T. Mizokawa, Robustness of excitonic coupling in Ta_2NiSe_5 against electronic inhomogeneity introduced by S substitution for Se, Adv. Quantum Technol. **6**, 2300034 (2023).

[10] G. Tomassucci, L. Tortora, G. Pugliese, F. Stramaglia, L. Simonelli, C. Marini, K. Terashima, T. Wakita, S. Ayukawa, T. Yokoya, K. Kudo, M. Nohara, T. Mizokawa, and N. L. Saini, Temperature dependent local inhomogeneity and magnetic moments of $(Li_{1-x}Fe_x)$OHFeSe superconductors, Phys. Chem. Chem. Phys. **25**, 6684 (2023).

[11] M. M. Traum, G. Margaritondo, N. V. Smith, J. E. Rowe, and F. J. DiSalvo, $TiSe_2$: Semiconductor, semimetal, or excitonic insulator, Phys. Rev. B **17**, 1836 (1978).

[12] M. Holt, P. Zschack, H. Hong, M. Y. Chou, and T. C. Chiang, X-ray studies of phonon softening in $TiSe_2$, Phys. Rev. Lett. **86**, 3799 (2001).

[13] F. Weber, S. Rosenkranz, J. P. Castellan, R. Osborn, G. Karapetrov, R. Hott, R. Heid, K. P. Bohnen, and A. Alatas, Electron-phonon coupling and the soft phonon mode in $TiSe_2$, Phys. Rev. Lett. **107**, 266401 (2011).

[14] H. Hughes, Structural distortion in $TiSe_2$ and related materials-a possible Jahn-Teller effect? J. Phys. C **10**, L319 (1977).

[15] M. Porer, U. Leierseder, J. Menard, H. Dachraoui, L. Mouchliadis, I. Perakis, U. Heinzmann, J. Demsar, K. Rossnagel, and R. Huber, Non-thermal separation of electronic and structural orders in a persisting charge density wave, Nat. Mater. **13**, 857 (2014).

[16] A. Kogar, M. Rak, S. Vig, A. Husain, F. Flicker, Y. Joe, L. Venema, G. MacDougall, T. Chiang, E. Fradkin, J. van Wezel, and P. Abbamonte, Signatures of exciton condensation in a transition metal dichalcogenide, Science **358**, 1314 (2017).

[17] S. Mathias, S. Eich, J. Urbancic, S. Michael, A. Carr, S. Emmerich, A. Stange, T. Popmintchev, T. Rohwer, M. Wiesenmayer, A. Ruffing, S. Jakobs, S. Hellmann, P. Matyba, C. Chen, L. Kipp, M. Bauer, H. C. Kapteyn, H. C. Schneider, K. Rossnagel, *et al.*, Self-amplified photo-induced gap quenching in a correlated electron material, Nat. Commun. **7**, 12902 (2016).

[18] E. Morosan, H. Zandbergen, B. Dennis, J. Bos, Y. Onose, T. Klimczuk, A. Ramirez, N. Ong, and R. Cava, Superconductivity in Cu_xTiSe_2, Nat. Phys. **2**, 544 (2006).

[19] S. Lee, T. B. Park, J. Kim, S. G. Jung, W. K. Seong, N. Hur, Y. Luo, D. Y. Kim, and T. Park, Tuning the charge density wave quantum critical point and the appearance of superconductivity in $TiSe_2$, Phys. Rev. Res. **3**, 033097 (2021).

[20] S. Kitou, A. Nakano, S. Kobayashi, K. Sugawara, N. Katayama, N. Maejima, A. Machida, T. Watanuki, K. Ichimura, S. Tanda, T. Nakamura, and H. Sawa, Effect of Cu intercalation and pressure on excitonic interaction in 1T-$TiSe_2$, Phys. Rev. B **99**, 104109 (2019).

[21] Y. Liu, D. F. Shao, L. J. Li, W. J. Lu, X. D. Zhu, P. Tong, R. C. Xiao, L. S. Ling, C. Y. Xi, L. Pi, H. F. Tian, H. X. Yang, J. Q. Li, W. H. Song, X. B. Zhu, and Y. P. Sun, Nature of charge density waves and superconductivity in 1T-$TaSe_{2-x}Te_x$, Phys. Rev. B **94**, 045131 (2016).

[22] H. Luo, W. Xie, J. Tao, I. Pletikosic, T. Valla, G. Sahasrabudhe, G. Osterhoudt, E. Sutton, K. Burch, E. Seibel, J. W. Krizan, Y. Zhu, and R. J. Cava, Differences in chemical doping matter: Superconductivity in $Ti_{1-x}Ta_xSe_2$ but not in $Ti_{1-x}Nb_xSe_2$, Chem. Mater. **28**, 1927 (2016).

[23] E. Morosan, K. E. Wagner, L. L. Zhao, Y. Hor, A. J. Williams, J. Tao, Y. Zhu, and R. J. Cava, Multiple electronic transitions and superconductivity in Pd_xTiSe_2, Phys. Rev. B **81**, 094524 (2010).

[24] A. Zunger and A. J. Freeman, Band structure and lattice instability of $TiSe_2$, Phys. Rev. B **17**, 1839 (1978).

[25] T. Kaneko, Y. Ohta, and S. Yunoki, Exciton-phonon cooperative mechanism of the triple-q charge-density-wave and antiferroelectric electron polarization in $TiSe_2$, Phys. Rev. B **97**, 155131 (2018).

[26] S. Kitou, T. Hasegawa, A. Nakano, N. Katayama, S. Tsutsui, and H. Sawa, Intercalated Cu ion dynamics in the two-dimensional layered compound $Cu_{0.33}TiSe_2$, Phys. Rev. B **101**, 094108 (2020).

[27] J. F. Zhao, H. W. Ou, G. Wu, B. P. Xie, Y. Zhang, D. W. Shen, J. Wei, L. X. Yang, J. K. Dong, M. Arita, H. Namatame, M. Taniguchi, X. H. Chen, and D. L. Feng, Evolution of the electronic structure of 1T-$Cu_x$$TiSe_2$, Phys. Rev. Lett. **99**, 146401 (2007).

[28] J. Jeong, J. Jeong, H. Noh, S. B. Kim, and H.-D. Kim, Electronic structure study of Cu-doped 1T-$TiSe_2$ by angle-resolved photoemission spectroscopy, Physica C **470**, S648 (2010).

[29] D. Qian, D. Hsieh, L. Wray, Y. Xia, R. J. Cava, E. Morosan, and M. Z. Hasan, Evolution of low-lying states in a doped CDW superconductor $Cu_x$$TiSe_2$, Phys. B: Condens. Matter **403**, 1002 (2008).

[30] M. Bendele, A. Barinov, B. Joseph, D. Innocenti, A. Iadecola, A. Bianconi, H. Takeya, Y. Mizuguchi, Y. Takano, T. Noji, T. Hatakeda, Y. Koike, M. Horio, A. Fujimori, D. Ootsuki, T. Mizokawa, and N. L. Saini, Spectromicroscopy of electronic phase separation in $K_xFe_{2-y}Se_2$ superconductor, Sci. Rep. **4**, 5592 (2014).

[31] T. Mizokawa, M. Bendele, A. Barinov, A. Iadecola, B. Joseph, T. Noji, Y. Koike, and N. L Saini, Mesoscopic stripes in antiferromagnetic Fe chalcogenide probed by scanning photoelectron spectromicroscopy, J. Phys. Soc. Jpn. **85**, 033702 (2016).

[32] T. Mizokawa, A. Barinov, V. Kandyba, A. Giampietri, R. Matsumoto, Y. Okamoto, K. Takubo, K. Miyamoto, T. Okuda, S. Pyon, H. Ishii, K. Kudo, M. Nohara, and N. L. Saini, Domain dependent Fermi arcs observed in a striped phase dichalcogenide, Adv. Quantum Tech. **5**, 2200029 (2022).

[33] T. Mizokawa, G. Tomassucci, M. Hattori, F. Minati, L. Tortora, A. Barinov, Z. Wang, J. X. Yin, and N. L. Saini, Electronic inhomogeneity in Cs- and Sb-terminated surfaces of CsV_3Sb_5 probed by scanning photoemission spectromicroscopy, Phys. Rev. B **112**, 075106 (2025).

[34] T. Sugimoto, E. Paris, K. Terashima, A. Barinov, A. Giampietri, T. Wakita, T. Yokoya, J. Kajitani, R. Higashinaka, T. D. Matsuda, T. Aoki, and N. L. Saini, Inhomogeneous charge distribution in a self-doped $EuFBiS_2$ superconductor, Phys. Rev. B **100**, 064520 (2019).

[35] T. Sugimoto, E. Paris, T. Wakita, K. Terashima, T. Yokoya, A. Barinov, J. Kajitani, R. Higashinaka, T. D. Matsuda, Y. Aoki, T. Mizokawa, and N. L. Saini, Metallic phase in stoichiometric $CeOBiS_2$ revealed by space resolved ARPES, Sci. Rep. **8**, 2011 (2018).

[36] F. Minati, G. Tomassucci, M. Hattori, Y. Fujita, M. Nagao, L. Tortora, A. Barinov, M. Kpciuszynski, G. Campi, L. Boeri, T. Mizokawa, and N. L. Saini, Intrinsic electronic structure and inhomogeneity of high-entropy layered $REOBiS_2$ superconductor, Inorg. Chem. **64**, 11260 (2025).

[37] A. Titov, A. Merentsov, A. Kar'kin, A. Titov, and V. Fedorenko, Structure and properties of the intercalation compound $Cu_x$$TiSe_2$, Phys. Solid State **51**, 230 (2009).

[38] S. Kitou, S. Kobayashi, T. Kaneko, N. Katayama, S. Yunoki, T. Nakamura, and H. Sawa, Honeycomb lattice type charge density wave associated with interlayer Cu ions ordering in 1T-$Cu_x$$TiSe_2$, Phys. Rev. B **99**, 081111(R) (2019).

[39] K. Momma and F. Izumi, VESTA3 for three-dimensional visualization of crystal, volumetric and morphology data, J. Appl. Crystallogr. **44**, 1272 (2011).

[40] P. Dudin, P. Lacovig, C. Fava, E. Nicolini, A. Bianco, G. Cautero, and A. Barinov, Angle-resolved photoemission spectroscopy and imaging with a submicrometre probe at the SPECTROMICROSCOPY-3.2L beamline of Elettra, J. Synchrotron Radiat. **17**, 445 (2010).

[41] P. Blaha, K. Schwarz, F. Tran, R. Laskowski, G. K. H. Madsen, and L. D. Marks, WIEN2k: An APW lo program for calculating the properties of solids, J. Chem. Phys. **152**, 074101 (2020).

[42] J. P. Perdew, K. Burke, and M. Ernzerhof, Generalized gradient approximation made simple, Phys. Rev. Lett. **77**, 3865 (1996).

[43] M. Huber, Y. Lin, G. Marini, L. Moreschini, C. Jozwiak, A. Bostwick, M. Calandra, and A. Lanzara, Ultrafast creation of a light-induced semimetallic state in strongly excited 1T-$TiSe_2$, Sci. Adv. **10**, eadl4481 (2024).

[44] R. Bianco, M. Calandra, and F. Mauri, Electronic and vibrational properties of $TiSe_2$ in the charge-density-wave phase from first principles, Phys. Rev. B **92**, 094107 (2015).

[45] H. J. Monkhorst and J. D. Pack, Special points for Brillouin-zone integrations, Phys. Rev. B **13**, 5188 (1976).

[46] O. Rubel, J. B. Moussy, P. Foulquier, and V. Brouet, Band unfolding with a general transformation matrix: From code implementation to interpretation of photoemission spectra, Comput. Phys. Commun. **291**, 108800 (2023).

[47] See Supplemental Material at http://link.aps.org/supplemental/10.1103/dg1f-hm99 for additional spectromicroscopy and space resolved ARPES data.

[48] M. Spera, A. Scarfato, E. Giannini, and C. Renner, Energy-dependent spatial texturing of charge order in 1T-$Cu_x$$TiSe_2$, Phys. Rev. B **99**, 155133 (2019).

[49] A. M. Novello, M. Spera, A. Scarfato, A. Ubaldini, E. Giannini, D. R. Bowler, and C. Renner, Stripe and short range order in the charge density wave of 1T-$Cu_x$$TiSe_2$, Phys. Rev. Lett. **118**, 017002 (2017).

[50] S. Yan, D. Iaia, E. Morosan, E. Fradkin, P. Abbamonte, and V. Madhavan, Influence of domain walls in the incommensurate charge density wave state of Cu intercalated 1T-$TiSe_2$, Phys. Rev. Lett. **118**, 106405 (2017).

[51] H. Cercellier, C. Monney, F. Clerc, C. Battaglia, L. Despont, M. G. Garnier, H. Beck, P. Aebi, L. Patthey, H. Berger, and L. Forro, Evidence for an excitonic insulator phase in 1T-$TiSe_2$, Phys. Rev. Lett. **99**, 146403 (2007).

[52] R. A. Jishi and H. M. Alyahyaei, Electronic structure of superconducting copper intercalated transition metal dichalcogenides: First-principles calculations, Phys. Rev. B **78**, 144516 (2008).

[53] C. Chen, B. Singh, H. Lin, and V. M. Pereira, Reproduction of the charge density wave phase diagram in 1T-$TiSe_2$ exposes its excitonic character, Phys. Rev. Lett. **121**, 226602 (2018).